SEDIMENT TRANSPORT AND BEACH TRANSFORMATION

Tomoya Shibayama, A.M. ASCE *

and

Kiyoshi Horikawa, M. ASCE **

ABSTRACT

Laboratory and field investigations were performed in order to formulate a predictive model of two-dimensional beach profile change. The observed transport was classified into six types, and transport formulas were deduced for each type based on a microscale description of sediment movement caused by wave action. A numerical model of two-dimensional beach transformation was then developed. Beach profile changes calculated with the model were then compared with the laboratory results. The model was found to give reasonable results except in the vicinity of the wave plunging point. The sediment transport calculation is based on a sinusoidal velocity profile. The model appeares to give good results as long as the wave motion can be reasonably approximated by linear wave theory.

1. INTRODUCTION

Surface waves traveling in shallow water over a sandy bed produce back and forth sand movement. Various attempts have been made to establish quantitative relationships for the sand movement and fluid motion. For example, Madsen and Grant (1976) found a clear relationship between a nondimensional averaged transport rate and the Shields parameter by extending the results of unidirectional flow sediment transport. However, in order to achieve the goal of developing a practical calculation method for sediment formula due to wave action, more precise observations are required to understand the complex mechanism of sediment movement. If the spatial and temporal variations of net sediment transport can be predicted, then two-dimensional beach transformation can be estimated. Here we report results of a study of the theoretical and empirical relationships of wave sediment transport and of two-dimensional beach profile change. The study is based on laboratory and field

 Research Associate, Dept. of Civil Eng., University of Tokyo, Bunkyo-ku, Tokyo 113 JAPAN
 ** Professor, Dept. of Civil Eng., University of Tokyo, Bunkyo-ku, Tokyo 113 JAPAN observations. The results are restricted to on-offshore sediment transport; longshore transport is left for future work.

The various topics of the investigation are presented in the following order. 1) A simple classification of sediment transport patterns based on the dominance of a bed load or a suspended load, and on the direction of the sediment transport is described; 2) A bed load formula is presented; 3) A formula for calculating the suspended load created by vortices in the vicinity of sand ripples is introduced; and 4) A simple quantitative model for predicting two-dimensional beach transformation is presented, and comparisons are made with laboratory results.

2. SEDIMENT TRANSPORT

2.1 Sediment transport types and classification

The bed configuration, in particular the presence of ripples, is considered to be one of the main factors necessary to suspend sand. The ripples also govern the sediment transport direction. Therefore, precise observations of sand movement and bed form patterns were made for a wide range of flow conditions in order to classify the sediment transport as a function of flow conditions.

The experiments were carried out both in a wave flume and in an oscillatory flow tunnel. The laboratory conditions are shown in Table 1. Well-sorted sands were used as bottom materials except for Cases 3 and 4 in the oscillatory tunnel, for which polystyrene particles were used. The sediment movement was recorded using either an 8-mm movie camera or a 16-mm high-speed motion analysis camera.

Field observations were carried out at Sabigahama Beach on Miyake Island, and at Ajigaura Beach and Oarai Beach, both in Ibaragi Prefecture, Japan. The field conditions are shown in Table 2. The transport mode was observed directly and recorded using an underwater 8-mm movie camera and an underwater 35-mm camera.

Based on both the laboratory and field observations, the sediment transport due to nearly sinusoidal wave action was classified according to predominance of bed load or suspended load, and according to the direction of sediment transport. We found it convenient to classify the sediment transport into six types as shown in Fig. 1.

1) Bed Load (BL): The bed is practically flat and no suspended sand clouds exist: sediment particles move along the bed surface. The direction of sediment transport is the same as the water flow.

2) Bed Load Suspended Load Transient (BST): Suspended sand clouds are formed above a rippled bed. Both bed load and suspended load exist.

Table 1: Laboratory conditions

WAVE	FLUME			
Case	Period (s)	Deep water wave height (cm)	Initial slope	Sand grain diameter (mm)
1	1.5	10.0	0.1	0.2
2	1.5	7.6	0.1	0.2
3	1.5	9.3	0.1	0.7
- ŭ	2.0	7.5	0.05	0.7
5	1.7	5.4	0.05	0.7
6	2.2	4.5	0.05	0.7
7	1.8	5.8	0.05	0.2

OSCILLATORY FLOW TUNNEL

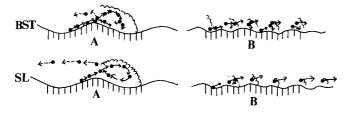
Case	Period (s)	Orbital diameter(m)	Particle diameter (mm)	Specific gravity
1	2.1 - 8.7	0.26 - 1.20	0.2	2.7
2	3.5 - 4.2	0.24 - 1.10	0.7	2.7
3	1.8 - 3.8	0.24 - 1.20	2.0*	1.4
4	2.9 - 7.1	0.22 - 0.70	0.3*	1.2
# Dolvetynone Dant		مار		

* Polystyrene Particles

Table 2: Field conditions

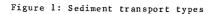
Case	Deep water wave height (m)	Period (s)	Sediment diameter (mm)	Date	Site
1	0.35	5	2	3 Nov 79	Sabigahama
2	0.3 - 0.45	7 - 8	10	24 Mar 80	Sabigahama
3	0.25 - 0.75	6 - 10	0.4 - 0.5	4 - 5 Jul 78	Ajigaura
4	0.25 - 0.50	4 - 10	0.2 - 0.3	28 Aug - 1 Sep 81	Oarai

BL



SF

Votation SUSPENDED SAND CLOUD SAND MOVEMENT DURING POSITIVE FLOW DIRECTION C----- SAND MOVEMENT DURING NEGATIVE FLOW DIRECTION



2-a) Ripple length and the water particle orbital diameter nearly equal (BST-A), sand particles suspended during the positively directed flow are first confined within a vortex, and then are transported towards the negative direction after the flow direction changes. We here use "positive" to indicate water flow direction in the first half wave period, and "negative" for the second half wave period. The transport of sediment which started moving during the first half wave period is either in the positive or negative direction depending on whether the bed load or suspended load is predominant.

2-b) Ripple length much smaller than the water particle orbital diameter (BST-B), sand particles suspended during positively directed flow are not confined within a vortex, and are therefore transported in the positive direction. Both suspended sand and sand moving along the bed move in the positive direction.

3) Suspended Load (SL): Suspended sand transport is predominant.

3-a) Ripple length and water particle orbital diameter nearly equal with sediment suspended during the first half wave period being transported in the negative direction (SL-A).

3-b) Ripple length much smaller than water particle orbital diameter with transport in the positive direction (SL-B).

4) Sheet Flow (SF): Ripples disappear. Sand particles move as a layer. The sediment transport direction is the same as the water flow.

In the SL and BST modes, the sediment transport direction changes depending upon the ratio of ripple length to water particle orbital diameter. The laboratory and field observations suggest that when the ripple length and the orbital diameter are of the same order, i.e., the latter is less than about three to five times the former, suspended sand clouds which were formed on the down-flow flanks of ripples are first confined witbin strong vortices. Then the sand clouds are transported in the negative direction during the period of negative flow, and are deposited on the bed under gravitational force (type A). When the ripple length is smaller than the water orbital diameter (i.e., the latter greater than about three to five times the former) suspended sand clouds formed on down-flow flanks of ripples are not confined in vortices and are transported in the positive direction during the period of positive flow (type B). In the BST mode, a part of the bed load is suspended to form sand clouds and some particles are .deposited on the bed immediately after suspension.

The above-described types were classified by means of three parameters as will now be described. In order to discuss the BL type, the initiation of sediment movement must be considered. Madsen and Grant (1976) analyzed laboratory data and found that the Shields parameter was an important descriptor. The Shields parameter is expressed in terms of the maximum value of the near bottom water velocity, and is defined as

$$\psi_{m} = \rho f_{w} u_{h}^{2} / 2(s-1)\rho g d$$

where f_W is Jonsson's (1966) wave friction factor, u_h the maximum value of near bottom velocity, s the sediment specific gravity, g the gravitational acceleration, ρ the fluid density and d the sediment diameter. Madsen and Grant showed that the critical value of Shields parameter corresponding to the initiation of sediment movement is a function of a quantity S. This quantity S depends only on the sediment and fluid properties, and is given by

$$S = d(s-1)gd/4v$$

where v is the kinematic viscosity of the fluid. For sediment particles of specific gravity 2.65 and diameter 0.2 to 2.0 mm, the critical value of Shields parameter is 0.03 to 0.05.

Komar and Miller (1975) analyzed laboratory data concerning initiation of ripple formation (under low shear stress) and the dissapearence of ripples (under high shear stress). They found that the limiting value of Shields parameter for the existance of ripples changes according to the sediment diameter. For sediment diameters 0.2 to 2.0 mm, the limiting value of Shields parameter for the disappearance of ripples varies from 0.4 to 0.8. However, in the present observation of the initiation of ripple formation, the critical condition was not sufficiently described by the Shields parameter and sediment diameter. The critical condition was also found to be a function of both time and the initial bottom configuration. The critical condition for the initiation of ripple formation is a very difficult problem.

The SL and BST transport types were further divided into two sub-types (A and B) depending upon the ratio of ripple length to water orbital diameter. Nielsen (1979) gave a functional relationship between this ratio and the nondimensional water velocity. According to his result, this ratio is nearly constant when the square of the dimensionless velocity, u_1^2 /(s-1)gd, is less than 25. Thus, sub-types A and B can be classified by using the square of the dimensionless velocity.

The parameter u_b/w is the ratio of maximum fluid velocity near the bed to the sediment particle fall velocity. Laboratory observation suggests that suspended sediment particles move at almost the same speed as the water particles. This implies that the parameter u_b/w is an indicator of the distance that a sediment particle travels when suspended. Thus the parameter u_b/w is related to suspended sediment movement.

The parameter $\psi_{\rm m}$ is related to the bed shear stress. Figure 2 shows the resulting classification of the laboratory and field data. This figure shows that the transport modes are well described by the two parameters, ${\rm u_b}/{\rm w}$ and $\psi_{\rm m}$.

For the limiting boundary between no-movement and BL, and BL and BST, the bed form pattern is the key factor, with the Shields parameter determining the transition. For BST and SL types, both u_h/w and ψ_m determine the limiting boundaries.

For the critical value for sub-types A and B of SL, a value of the square of the dimensionless velocity equal to 25 roughly corresponds to a value of the Shields parameter $\psi_{\rm m}$ in the range 0.125 to 0.25, if the wave friction factor is 0.01 to 0.02. An example with the value $\psi_{\rm m}$ = 0.19, which corresponds to f_W = 0.015, is also indicated in Fig. 2 (labelled "Nielsen").

It should be noted that the transition from SL-A to SL-B cannot be clearly classified by the dimensionless velocity alone. The transition is also related to the water orbital diameter. When the orbital diameter increases, the mode SL-B appears at lower velocities. Due to the same reason, the BST-B type appears when the water orbital diameter becomes longer than the ripple wave length.

4

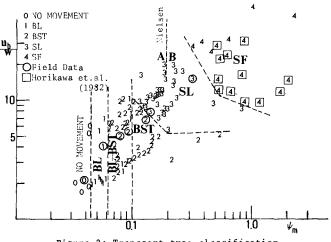


Figure 2: Transport type classification

2.2 Bed load

Vincent (1957) and Abou-Seida (1965) measured the bed load transport rate in a wave flume. Manohar (1955), Kalkanis (1962), and Abou-Seida (1965) performed experiments using an oscillatory plate in a tank of still water. In these experiments, the sediment was collected in a sampler which was set into the bed and the average transport rate over one wave period was evaluated. No consideration of transport direction was included. Sleath (1978) used an oscillatory plate and measured the quantities of bed material in motion at each instant of a cycle. Horikawa et al. (1977) measured the bed load using a sand trap which was buried in the bottom of a wave flume. They correlated the results with the beach profile chauge. Madsen and Grant (1976) proposed an empirical relationship between a dimensionless time averaged rate of sediment transport and the Shields parameter, based on analyzing the laboratory data of Kalkanis (1962) and Abou-Seida (1965). They used a quasi-steady application of the Einstein-Brown sediment transport relationship and Jonsson's (1966) wave friction factor, and obtained an expression for the bed load transport rate due to sinusoidal wave motion. In the present work, experiments were performed to measure quantities of sand in motion and the water particle velocity at each instant of the wave cycle in a flume. The results were compared with a formula derived by modifying the Madsen-Grant transport formula. The Madsen-Grant formula, which was based on an analogy of quasi-steady undirectional bed load transport, was supported by the present experiments which measured the history of sand transport rate within one wave period.

Madsen and Grant (1976) used a quasi-steady assumption with Brown's formula and obtained a similar relationship for oscillatory flow, namely,

$$\Phi(t) = 40 \psi'(t)$$
 (2)

$$\psi(t) = \tau(t) / (s-1)\rho gd$$
 (3)

in which Φ is the dimensionless sediment transport rate, ψ is the Shields parameter, and τ is the bed shear stress.

Assuming a sinusoidal velocity change, they obtained a relationship between the time-averaged dimensionless transport rate and the Shields parameter as

$$\overline{\Phi} = 12.5 \psi_{\rm m}^3 \tag{4}$$

in which

$$\overline{\Phi} = \overline{q}$$
 / wd (5)

$$\psi_{\rm m} = \tau_{\rm m} / (s-1)\rho g d \tag{6}$$

where \overline{q}_{s} is the time-averaged volumetric rate of sediment transport and w is the sand particle fall velocity. The quantity $\tau_{\rm m}$ is the maximum bed shear stress given by

$$\tau_{\rm m} = f_{\rm W} \rho \, u_{\rm b}^2 / 2$$
 (7)

We now use the observation that a sand particle moving as bed load will not stop until the flow direction changes. When sand particles are accelerated, the transport rate is estimated with Eq. (2). Assuming a sinusoidal velocity change, we get

$$\Phi(t) = 40 \psi_{\rm m}^3 \sin^0 \sigma t \tag{8}$$

in which $\sigma = 2\pi/T$, where T is the wave period. For the time interval after the volume of moving sand attains a maximum, sand

particles once started in motion will not stop during the interval. We have

$$\Phi(t) = \Phi_{m} u(t) / u_{h}$$
(9)

in which Φ_m is the maximum value of transport rate. Assuming a sinusoidal velocity change,

$$\Phi(t) = 40 \,\psi_m^3 \sin\sigma t \tag{10}$$

The transport rate averaged over the first half wave period is thus estimated from

$$\overline{\Phi} = 2\left(\int_{0}^{T/4} 40 \,\psi_{\rm m}^{3} \sin^{6}\sigma \,t \,dt + \int_{T/4}^{T/2} 40 \,\psi_{\rm m}^{3} \sin\sigma \,t \,dt\right) \,/{\rm T} \quad (11)$$
$$= 19 \,\psi_{\rm m}^{3}$$

Experiment 1 was performed in a wave flume 11 m long, 0.2 m wide, and 0.3 m deep. In the middle of the flume, a volume of sand was placed 0.04 m deep and 0.8 m long over the full flume width. Sand samples were well sorted and their median grain size was 0.7 mm. The wave conditions were as follows: wave height in the inspection section was 7.1 to 10.7 cm, wave period 0.94 to 1.44 s, and water depth 15.4 to 16.7 cm.

During the experiment runs, no sand ripples formed and the sand was transported as bed load. Polystyrene particles of diameter 2 mm and specific gravity 1.02 were injected into the water to measure the water particle movement. In order to measure the number of moving sand particles, a flat plate 2 cm long with a skirt to prevent local erosion was installed on the sand surface. The movement of sand particles which crossed the plate, and the motion of the polystyrene particles over the section, were observed using a CANON 16-mm movie camera utilizing a film speed of 48 frames per second. The relation between the wave phase and the film was determined by using a timing light system with a wave gage. The number of sand particles which crossed the section and the polystyrene particle movement was obtained by analyzing the 16mm film. The near bottom velocity was then estimated from the movement of the polystyrene

An example of the results obtained in Experiment 1 is compared with calculated values of the instantaneous transport rate in Fig. 3. The surface profile, the near bottom velocity and the number of the sand particles crossing the section at each instant of a wave period are shown in the figure. Sand particles did not start moving until the Shields parameter exceeded 0.05. When the transport rate was calculated from the velocity records, it was assumed to be zero when the motion was accelerated, and the instantaneous Shields parameter was less than 0.05. When the motion decelerated and the Shields parameter fell below 0.05, the transport rate was not taken to be zero because particles can continue in motion. Using Eqs. (2) and (9), a value of the sand flux was calculated.

As seen in Fig. 3, which is a representative result from thirteen runs, the agreement between the calculated and the measured values indicates the validity of the calculation scheme. The result also indicates that when the fluid decelerates, Eq. (9) gives a better approximation than Eq. (2) alone. However the real physical phenomena appears to be described by some intermediate combination of the two equations. From the laboratory observations, as the wave period becomes shorter, Eq. (9) becomes more applicable. The present model (Eqs. (2) and (9)) also seems to give a better estimate than Eq.(2) alone of the average transport rate integrated over the period of onshore flow direction.

2.3 Suspended load

Hom-ma and Horikawa (1963) measured auspended sediment concentrations and interpreted the results with a diffusion equation approach. Nakato et al. (1977) studied sediment concentration and velocity fluctuations using an Iowa-type concentration meter and a hot-film anemometer. The above

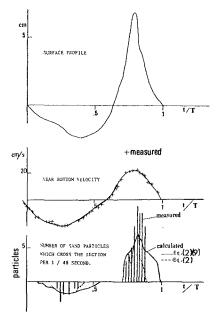


Figure 3: Result of Experiment1

two experiments concern the concentration distribution. Nielsen (1979) attempted to calculate the suspended load using the product of concentration and velocity distributions, but the results were far from satisfactory.

Concerning sand movement above a rippled bed, Inman (1957) studied ripple formation and suggested that suspended sand cloud formation is an important factor in considering sediment transport due to waves. Inman and Bowen (1971) found that there exists an offshore sand transport as suspended load due to ripple asymmetry and resulting differences in intensity of the vortices. Sunamura, et al. (1978) observed sand movement over ripples and described precisely how the sand is confined within vortices formed behind sand ripples and moved by the wave oscillatory flow.

Here, the rate of sand suspension is estimated by application of the Madsen-Grant transport formula and is compared with laboratory data. When strong vortices are created on the onahore sides of ripples, suspended sand clouds form. When the flow velocity is in the onshore direction, sand is transported along the offshore flanks of the ripples as bed load and then suspended at the crests of the ripples. The suspended sand forms a suspended sand cloud as shown in Fig. 4. Because of the ripple asymmetry, vortices created on the offshore sides of the ripples are weak. For our purposes, a strong vortex is taken as a circulation strong enough to produce suspended sand clouds. From here on, only strong vortices will be treated.

We now consider the time interval $t_j \leq t \leq t_g$ during which suspended sand clouds are formed. The time t_j indicates the time when clouds start to form and t_g indicates they stop increasing in size. The time average transport rate for a half wave period is estimated in the same manner as bed load to be

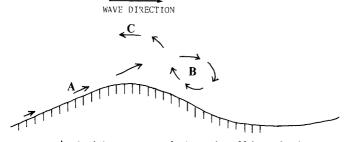
$$\overline{\Phi} = 80 \psi_m^3 \left(\int_{t_i}^{T/4} \sin^6 \sigma t \, dt \right) + \int_{T/4}^{t_e} \sin \sigma t \, dt \right) / T$$

$$= C \psi_m^3 \qquad (13)$$

From the laboratory observation, suspended sand cloud formation starts at 0.05T to 0.15T and ends at 0.45T to 0.5OT. Therefore the constant C varies from 16 to 19. We here set $t_{\rm i}$ = 0 and $t_{\rm g}$ = 0.5T which gives the maximum value of C. Equation (13) then becomes

$$\overline{\Phi} = 19 \psi_{\rm m}^3 \tag{14}$$

Experiment 2 was performed to study suspended load. The same flume was used as in Experiment 1 for bed load. In the middle of the flume, a volume of sand was placed which was 4 cm thick, 80 cm long and 20 cm wide. Sand samples were well sorted and their median grain size was 0.2 mm. The wave height was 5.8 to 8.3 cm, and the period 0.84 to 1.30 s.



A: Sand is transported along the offshore flank of the ripples

- B: Sand forms a suspended sand cloud
- C: The cloud is transported in the offshore direction

Figure 4: Formation of suspended sand cloud

ş

When waves were generated, sand ripples formed after 200 to 300 wave periods. The resultant ripple lengths were 3.0 to 5.7 cm and the height were 0.35 to 0.90 cm. The ripples were asymmetric and strong vortices were generated on the onshore sides of the ripples; vortices formed on the offshore sides were much weaker.

In order to obtain the rate of sand suspension at the crests of ripples, the distribution of suspended sediment concentration above the rippled bed must be measured. A concentration meter was installed close to the bed. It could measure the spatially averaged concentration of the suspended sand clouds. Here, the same assumption as Sunamura et al. (1979) was applied. They assumed that the concentration within the cloud is homogeneous. This assumption is reasonable because of the strong mixing effects of vortices. This condition was seen in precise observations of sand movement by Sunamura et al. and in the present experiment. The concentration was formed.

The concentration of the clouds was measured with a KENEK suspended sand concentration meter which optically measures the suspended sand concentration. The output of the meter was recorded on oscillograph paper together with the output of the wave gage. The cross-sectional area of the suspended sand cloud was obtained from 16-mm films. The amount of suspended sand in the cloud was estimated as the product of the concentration and the cross-sectional area of the cloud.

The results for the rate of sand suspension are shown in Fig. 5 together with the laboratory data of Sunamura, et al. (1979), and a more recent result, Sunamura (1982). Sunamura (1979, 1982) directly determined the net sediment transport rate by measuring the sand weight. The agreement between Eq. (14) and the laboratory data is good. This result implies that the suspended load can be estimated by Eq. (14) for the bed load moving along the ripple flanks.

2.3 Sediment tansport formulas

Simple formulas for the six types of sand transport are now given using the above results. The description of the suspended load requires the introduction of two quantities. The quantity α is the ratio of suspended load originating from the bed load to the bed load. The quantity β is the ratio of suspended sediment confined by a vortex to the suspended sediment. These two quantities are a function of sediment diameter, specific gravity, near bottom velocity, ripple geometry, vortex circulation, etc. Figure 6 shows a schematic diagram for the two parameters.

For type BL, Eq. (6) is used directly. For type SL-A, Eq. (14) is used taking into consideration the number of ripple lengths the suspended sand clouds travel in the second half wave period. Therefore the quantity N is introduced, which is the maximum integer not exceeding the quantity D/λ , where D is the orbital diameter of water particles and λ the ripple wave length. Thus N indicates how many ripple lengths the cloud travels during a half wave period. We then obtain the formula

$$\overline{\Phi} = -19N \psi_{\rm m}^3$$

(15)

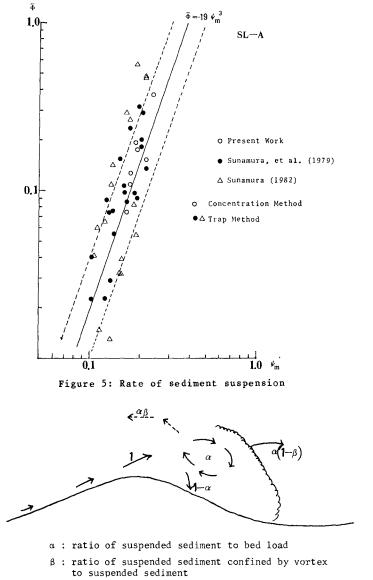


Figure 6: Explanation of two parameters

Figure 7 shows a comparison between Eq. (15) and the laboratory results. Good agreement is seen. In type BST-A, a part of the bed load is suspended to form clouds and some of the sand particles are deposited on the bed immediately after suspension. We obtain

$$\overline{\Phi} = (1 - \alpha) 19 \psi_{\rm m}^3 - 19\alpha N \psi_{\rm m}^3 = (1 - \alpha - N\alpha) 19 \psi_{\rm m}^3 \qquad (16)$$

for type BST-A. Values of a must be determined empirically. For types SL-B and BST-B, the suspended sand clouds formed along the down-flow flanks of ripples are transported in the same direction as the water flow. The formula for type SL-B and BST-B is

$$\overline{\Phi} = 19 \psi_m^3$$

For type SF, Horikawa et al. (1982) performed experiments to determine transport rate. As shown in Fig. 8, Eq. (11) fits their data.

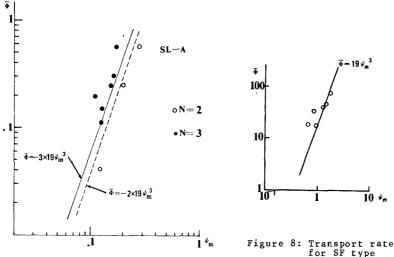


Figure 7 : Comparison with laboratory data, SL-A type

(17)

Figure 9 shows the six types of transport and their respective calculation. Although the results are too simple for general use at present, the approach of reducing the complex phenomena into simpler divisions as done here is considered to be promising.

3. TWO-DIMENSIONAL BEACH TRANSFORMATION

The transport formulas derived in the previous section are now applied to predicting beach profile change by comparing the calculation with laboratory results.

Many works had been done to analyze two-dimensional beach transformation. For example, Johnson (1949) classified beach profiles into bar and step types and first gave governing parameters by which beach type can be classified. Eagleson et al. (1963) were the first to attempt to calculate beach profile change, but the calculated results did not agree with the measured results. This is probably because they did not consider the effect of ripples. In this study, beach profile change will be discussed based on the sediment transport mechanism of ripples.

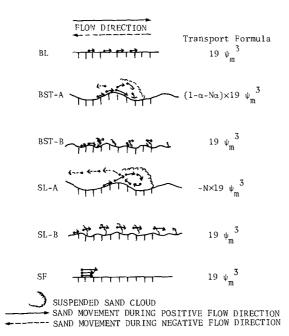


Figure 9: Sediment transport formula

In the present calculation, the above transport formulas were applied to the entire area of the beach because the same transport mechanism was observed in most areas (e.g., the transport in the breaking region was different and therefore an exception). Figure 10 shows the procedure of the computer simulation. The calculation can be started from an arbitrary initial beach profile. Wave transformation and velocity fields are calculated from the incident wave condition and bottom profile. Using the above results, the sediment transport rate can be calculated. Then the beach profile change can be calculated using the continuity equation for bed material.

In order to calculate, the following assumptions were made based on the laboratory and field investigations (see Fig. 11):

1) The wave transformation is given by linear wave theory using incident wave conditions and water depth in the offshore region. The wave breaking condition is given by Madsen (unpublished lecture notes) as

$$H_b/L_b = 0.142 \, tanh \left[(0.8 + 5i) \, 2\pi h_b / L_b \right]$$
(18)

where H_h is the breaking wave height, and L_b is the wave length at the breaking point. The wave height after breaking is assumed to decrease proportionate to the distance between the breaking point to the maximum run-up point. The run-up height, R, from the still water level is given by Hunt (1959) to be

$$R = 1.01 i \sqrt{H_0 L_0}$$

where i is the beach slope.

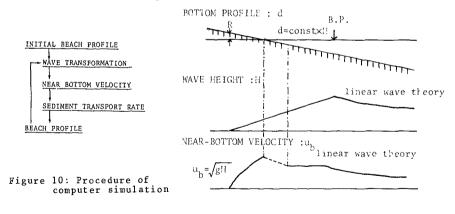


Figure 11: Assumptions for simulation

.....

(19)

2) The maximum value of the near-bottom velocity is calculated from linear wave theory using the wave height and water depth where the wave height is less than the water depth (Region 1). In the swash zone, where beacb surface is situated above the still water level (Region 2),

 $u_b = \sqrt{gH}$

(20)

(21)

is adopted as suggested by Ogawa and Shuto (1981). Here H is the local wave height. In the transition zone between Regions 1 and 2, the maximum velocity is assumed to change proportional to the distance from Region 1 to 2.

3) The sediment transport rate is calculated from the formulas in the previous section. Due to the non-linear effect of wave motion over gently sloping beaches, the maximum value of the water velocity in the onshore direction is greater than that in the offshore direction. From observation in the laboratory, the transport rate of sand which started moving during the onshore directed flow is much larger than the sand which stared moving during offshore directed flow. Therefore, we calculate only the sand which started moving during onshore directed flow. The value for BST type transport is calculated assuming a linear relationship with the Shields parameter. This means that the value changes from 0 to 1 proportionate to the Shields parameter in the area of BST transport type; i.e., $a = (\psi_m - \psi_1)$ $/(\psi_2 - \psi_1)$, where ψ_2 is the maximum Shields parameter which corresponds to BST transport type for specific u_h/w , and ψ_1 is taken as the minimum value in Fig. 2. In order to calculate the parameter N, the ripple wave length was obtained from an expression given by Nielsen (1979):

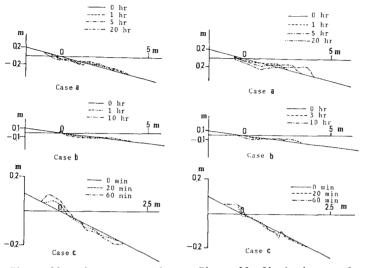
$$\lambda / D = 1.1 - 0.172 \left[u_b^2 / (s-1)gd \right]^{0.34}$$

The time step for the calculation is selected to be 6 s for a step-type and 1 min. for a bar-type beach. This was found acceptable for the present condition. When beach profile was calculated from transport rate, beach profile was smoothed if transport rate rapidly changed comparing with those of vicinity places.

Three sets of laboratory experiments were performed to examine the model. During the experiments, bottom profile change, suspended sediment concentration, near bottom velocity and surface profile were measured. In order to measure the near bottom velocity, polystyrene particles were injected and a 16-mm camera was used to record the movement of this tracer.

Figure 12 shows the laboratory results of beach profile change. Figure 13 shows the results of the simulation. The two results show reasonable agreement. Figures 14 and 15 give detailed comparisons of the wave height, near bottom velocity, transport rate and beach profile change.

The prediction with this model gave a good approximation to the profile change in the offshore region, but the estimate was not so good in the surf zone. This is mainly caused by the fact that in the surf zone, pure sinusoidal wave motion is no longer present, and the effect of wave breaking is very strong. The agitation due to breaking waves suspends the bed material, and the concentration of the suspended sediment in the vicinity of breaking point is high. In order to improve this model, the velocity field in the surf zone should be evaluated more precisely. A study based on this point of view was made by Shibayama and Horikawa (1982).





5. CONCLUSIONS

The main results of the present study are as follows:

1) Sediment transport can be classified into six types according to whether bed load or suspended load is predominant, and according to the sediment transport direction.

2) The transport type can be classified by three parameters, the Shields parameter, the ratio of maximum fluid velocity to sediment particle fall velocity, and the ratio of water particle orbital dismeter to ripple wave length.

3) By using certain assumptions and empirical information, bed load and suspended load under waves can be estimated by expressions originally derived for unidirectional bed load transport.

4) Net sediment transport formulas were developed. These expressions were applied to predict two-dimensional beach profile change in the laboratory. Reasonable agreement was obtained in regions where the wave motion can be reasonably approximated by linear wave theory.

ACKNOWLEDG EMENT

The authors thank Dr. N. C. Kraus of the Nearshore Environment Research Center for his advice in correcting an early version of the manuscript.

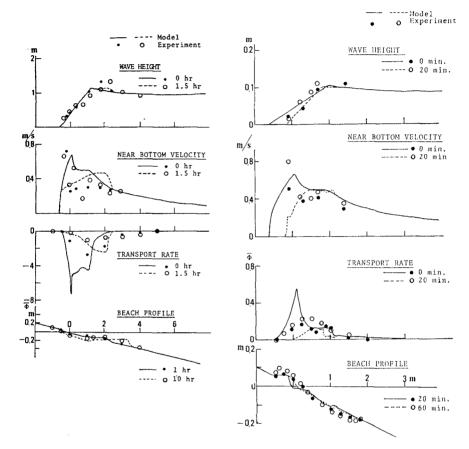


Figure 14: Comparison of model and measured value, Example a

Figure 15: Comparison of model and measured value, Example b

REFERENCES

1) Abou-Seida, M. M. :"Bed load function due to wave action," Univ. of Cal., Berkeley, Hydraulic Eng. Lab., HEL-2-11, 78pp., 1965.

2) Dingler, J. R and Inman, D.L. :"Wave-formed ripples in nearshore sands," Proc. 15th Coastal Eng. Conf., pp. 2109-2126, 1976.

3) Eagleson, P.S., Glenne, B and Dracup, J.A. :" Equilibrium characteristics of sand beaches," Proc. ASCE, Vol. 89, No. HY1, pp. 35-37, 1963.

4) Hom-ma, M and Horikawa, K., :"Suspended sediment due to wave action," Proc. 8th Coastal Eng. Conf., pp. 108-193, 1963.

5) Horikawa, K., Sunamura, T. and Shibayama, T. :"Experimental study of two-dimensional shore transformation," Proc. 24th Japanese Conf. on Coastal Eng., pp. 170-174, 1977 (in Japanese).

6) Horikawa, K., Watanabe, A., and Katori, S., :"Sediment transport under sheet flow condition," Proc. 18th Conf. on Coastal Eng., 1982 (in press).

7) Inman, D. L. and Bowen, A. J., :"Flume experiments on sand transport by waves and currents," Proc. 8th Coastal Eng. Conf., pp. 137-150, 1963.

8) Johnson, J. W. :"Scale effects in hydraulic models involving wave action," Trans., A.G.U., Vol.30, pp. 517-525, 1949.

9) Jonsson, I. G. : "Wave boundary layers and friction factors," Proc. 10th Coastal Eng. Conf., Vol.1, pp. 127-148, 1964.

10) Kalkanis, G. :"Transport of bed materials due to wave action," CERC, Tech. Memo. No.2, 38 pp., 1964.

11) Komar, P. D. and Miller, M. C. :"The initiation of oscillatory ripple marks and the development of plane-bed at high shear stresses under waves," Jour. of Sedimentary Petrology, Vol.45, No.3, pp. 697-703, 1975.

12) Madsen, O.S. and Grant, W.D. :"Quantitative description of sediment transport by waves," Proc. 15th Coastal Eng. Conf., pp. 1093-1112, 1976.

13) Manohar, M. :"Mechanics of bottom sediment movement due to wave action," BEB Tech. Memo. No. 75, 121 pp., 1955.

14) Nakato, T., Locher, F. A., Glover, J.R. and Kennedy, J.F. "Wave entrainment of sediment from rippled beds," Proc. ASCE, Vol. 103, No. WW1, pp. 83-99, 1977. 15) Nielsen, P. :"Some basic concepts of wave sediment transport," Series Paper No.20, Tech. Univ. of Denmark, 160 pp., 1979.

16) Ogawa, Y. and Shuto, N. :"On the dynamics in surf zone," Proc. of 29th Japanese Conf. on Coastal Eng., pp. 135-140, 1982 (in Japanese).

17) Shibayama, T. and Horikawa, K. :"Laboratory study on sediment transport mechanism due to Wave action," Proc. JSCE, No.296, pp. 131-142, 1980-a.

18) Shibayama, T. and Horikawa, K. :"Bed load measurment and prediction of two-dimensional beach transformation," Coastal Eng. in Japan, Vol. 23, pp. 179-190, 1980-b.

19) Shibayama, T. and Horikawa, K. :"Sediment suspension due to breaking waves," Coastal Eng., in Japan, Vol. 25, 1982 (in press).

20) Sleath, J.F.A. : "Measurement of bed load in oscillatory flow," Proc. ASCE, Vol. 104, No. WW4, pp. 291-307, 1978.

21) Sunamura, T., Bando, K. and Horikawa, K. :"Experimental study of sand movement and transport over asymmetrical ripples," Proc. 25th Japanese Conf. on Coastal Eng., pp. 250-254, 1978 (in Japanese).

22) Sunamura, T. :"On-offshore sediment transport in shallow water region," Proc. 29th Japanese Conf. on Coastal Eng., pp. 239-243, 1982 (in Japanese).

23) Vincent, G.E. :"Contribution to the study of sediment transport on a horizontal bed due to wave action," Proc. 6th Coastal Eng. Conf., pp. 326-354, 1958.